Available online at www.sciencedirect.com
SCIENCE DIRECT®
Surface Science 532–535 (2003) 1092–1097
SURFACE SCIENCE
www.elsevier.com/locate/susc

Electrochemical preparation of lead-doped amorphous Se films and underpotential deposition of lead onto these films

Dmitry K. Ivanov [a,*], Nikolay P. Osipovich [b], Sergey K. Poznyak [b], Eugene A. Streltsov [a]

[a] *Chemical Department, Belarusian State University, Leningradskaya st. 14, Minsk 220050, Belarus*
[b] *Institute of Physico-Chemical Problems, Belarusian State University, Leningradskaya st. 14, Minsk 220050, Belarus*

Abstract

The process of the underpotential deposition (UPD) of Pb adatoms (Pb_{ad}) onto Se was used to produce nanocomposite films consisting of amorphous Se and nanosized PbSe clusters distributed throughout the film bulk. It was found that doping lead into Se films modifies their optical and photoelectrochemical properties and increases the efficiency of the charge transfer both in the film bulk and through the semiconductor | electrolyte interface. Introducing lead into the bulk of Se films significantly promotes the process of Pb_{ad} UPD onto Se surface. The underpotentially deposited Pb_{ad} interact chemically with Se surface atoms, resulting in the formation of a PbSe monolayer. The PbSe formed can be identified by the anodic peak corresponding to its electrochemical oxidation.

Keywords: Electrochemical methods; Chalcogens; Lead; Amorphous thin films; Adatoms; Semiconductor–electrolyte interfaces; Semiconductor–semiconductor thin film structures

1. Introduction

The study of the underpotential deposition of metals onto the surface of semiconductor electrodes is of interest for electrodeposition of textured [1] and epitaxial films [2–8], electrosynthesis of metal chalcogenides [9–12] and superlattice structures [13,14]. In the past decade, an additional interest in the underpotential deposition (UPD) processes has been stimulated by the progress in studying the physics and chemistry of nanosized objects and has been associated with revealing the peculiarities of the electron properties of nanolayers, which differ from those of bulk objects.

We have recently reported on the possibility of the photoinduced UPD of Pb_{ad} onto polycrystalline Se electrodes with p-type conductivity [15]. In the dark, the UPD of Pb_{ad} onto Se surface does not occur because of the extended space charge region (SCR) being formed, which hinders the charge transport through the Se | electrolyte interface. On illumination, electron–hole pairs photogenerated in Se are separated by the field in the SCR. Photoelectrones move towards the electrode surface and reduce the Pb^{2+} ions, resulting in the photoinduced UPD of Pb_{ad} on selenium. The interaction of the Pb adatoms with Se matrix can result in the formation of PbSe clusters at the surface. Once the Se surface has been modified by

* Corresponding author. Tel.: +375-182-239400; fax: +375-172-264-696.
E-mail address: elchem@bsu.by (D.K. Ivanov).

0039-6028/03/$ - see front matter
doi:10.1016/S0039-6028(03)00218-8

nanosized PbSe clusters promoting the charge transfer through the semiconductor | electrolyte interface, the UPD process becomes possible [15].

In the present work, amorphous Se films with lead doped in their bulk owing to the UPD process were prepared. Their structure as well as the optical, electro- and photoelectrochemical properties were studied, and the effect of lead doping on the electrochemical activity of Se in the Pb UPD process was examined and discussed.

2. Experimental

2.1. Film preparation

Amorphous selenium films and Se films doped with lead were formed electrochemically on the surface of Au foil electrodes. For optical measurements, those films were deposited onto conducting ITO films on a glass sheet. Amorphous Se was deposited potentiostatically (−0.3 V) in electrolyte containing 0.02 M SeO_2 + 0.1 M HNO_3 ($T = 20$ °C) for 30 min under illumination with a 150 W halogen lamp ($J = 40$ mW cm^{-2}).

Lead-doped Se films (Se(Pb)) were produced potentiostatically in the dark in a similar solution containing $Pb(NO_3)_2$. The Pb/Se ratio in the films was varied by changing the Pb^{2+} concentration in solution from 2×10^{-5} to 2×10^{-3} M and by changing the electrode potential from −0.1 to −0.3 V. The thickness of the Se and Se(Pb) films estimated from their elemental analysis with allowance made for the density of amorphous Se (4.28 g cm^{-3}) was found to be about 0.1 μm.

PbSe thin films used for comparison with the Se(Pb) ones were deposited onto an Au electrode from 1 M $Pb(NO_3)_2$ + 0.001 SeO_2 + 0.1 M HNO_3 solution under potentiostatic polarization at $E = -0.3$ V for 30 min. These films are polycrystalline and have the composition: 49 ± 1 at.% Pb and 51 ± 1 at.% Se.

2.2. Apparatus and chemicals

Electrochemical and photoelectrochemical measurements were carried out in a standard three-electrode cell equipped with an optical quality window, a platinum counter-electrode and a saturated $Ag|AgCl|KCl_{(sat)}$ electrode as the reference one (+0.201 V vs. SHE). All potentials were controlled by a conventional potentiostat with a programmer and determined with respect to this reference electrode. Photocurrent spectra were recorded using a set-up equipped with a high intensity grating monochromator, a 1000 W Xe lamp and a slowly rotating light chopper (0.3 Hz). The photocurrent spectra were corrected for the spectral intensity distribution at the monochromator output.

Optical spectra were measured using a Specord M40 UV-Vis spectrometer (Carl Zeiss, Jena). AFM images were obtained with a FemtoScan-001 microscope (Advanced Technologies Center, MGU, Moscow) operated in the constant force mode (1.5–5 nN) under ambient conditions. X-ray diffraction analysis of the films was performed on a HZG-4A diffractometer (Cu-K_α radiation, Ni filter). The Pb content in the films was determined after the film dissolution by AES method using a Spectroflame Modula atomic emission spectrometer.

All chemicals used were of analytical grade or of the highest purity available. The solutions were prepared using doubly distilled water.

3. Results and discussion

3.1. Electrochemical formation of Pb-doped amorphous Se films

During the cathodic deposition of Se films in the dark under potentiostatic control (potentials from 0 to −0.4 V were applied) in 0.02 M SeO_2 + 0.1 M HNO_3 solution, the current drops sharply with time (by 90% in 30 s). The film growth virtually stops after 5 min deposition. This effect is related to the fact that Se has a low p-type conductivity and cuts off the cathodic current. The thickness of the films deposited under those conditions did not exceed 10 nm.

Adding Pb^{2+} ions into the electrolyte eliminates the problems associated with the current cut-off and makes it possible to deposit films with the thickness up to several micrometers. We carried

out the film deposition at potentials more positive than the Pb^{2+}/Pb reversible potential. Under these conditions, selenium is deposited with an overvoltage in the regime of the limiting diffusion current, and lead is co-deposited due to the UPD process on Se [9]. The potential region from −0.1 to −0.3 V is suitable for the deposition of both Pb adatoms and Se monolayers on the Au electrode surface. It is important to note that early in the process of Se(Pb) film growth, the Pb UPD occurs both at the Au surface and at the Se monolayer surface, because this process is possible on the Se monolayer unlike the case of the bulk Se films [10]. Further co-deposition of Pb and Se proceeds at the surface of the Pb-doped Se films.

The Pb content in the deposited Se(Pb) films varies in the range from 1 to 30 at.% and increases with Pb^{2+} concentration in solution or when the electrode potential is shifted to more negative values.

3.2. Structure and morphology of Se and Se(Pb) films

X-ray diffraction analysis showed that the undoped Se film and Se(Pb) films with the Pb content <5 at.% are amorphous. At higher Pb content, XRD peaks of the PbSe phase appear (Fig. 1). These peaks are strongly broadened, which is indicative of a high-disperse state of PbSe. The average size of PbSe crystallites estimated from the XRD peaks' half-width is 2–4 nm.

AFM images of the film surface demonstrate that introducing lead into the Se film results in the appearance of a distinct globular structure. The specific surface area of the Se(Pb) films increases with increasing the Pb content. The average size of the globules for the Se(Pb) films (8 at.% Pb) is 200–300 nm.

3.3. Optical, electro- and photoelectrochemical properties of Se and Se(Pb) films

Fig. 2(a) shows spectral dependences of the absorption coefficient (α) for the undoped Se films and Se films doped with 1 and 3 at.% Pb. The spectrum of Se has a wide region of the exponential rise of α in the photon energy range from 1.7 to 2.2 eV (so-called Urbach tail), which is characteristic of amorphous semiconductors.

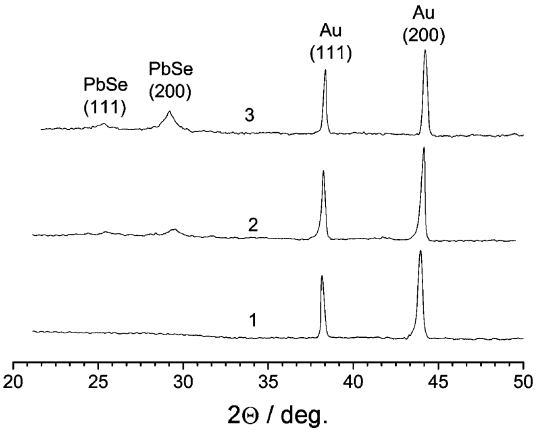

Fig. 1. X-ray diffraction patterns for the Pb-doped Se films (1 at.% Pb (1), 8 at.% Pb (2) and 11 at.% Pb (3)) electrodeposited at an Au substrate.

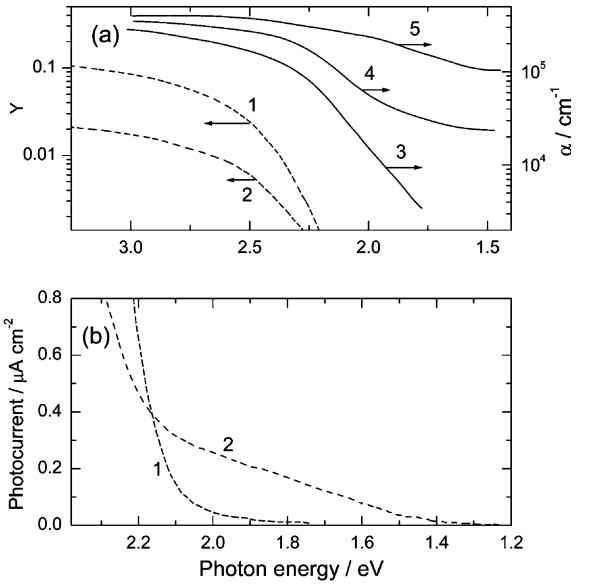

Fig. 2. (a) Absorption (—) and photocurrent quantum yield (- - -) spectra of the undoped selenium film (1, 3) and Pb-doped Se film (1 at.% Pb (2, 4) and 3 at.% Pb) (5). Photocurrent spectra were measured in 0.1 M HNO_3 solution at a potential of −0.2 V. (b) Long-wavelength edge of the photocurrent spectra of the undoped (1) and Pb-doped (1 at.% Pb) (2) selenium films.

Introducing lead into the Se films results in a significant rise of the absorption in the long-wavelength region of the spectrum, where amorphous Se absorbs negligibly. Furthermore, some shift of the Urbach edge (by 0.1 eV) to lower energies is observed (Fig. 2(a)). Such changes in the optical properties of Se films on the lead doping can be due to a number of reasons. At low doping levels, impurity atoms can cause an increase in the localized electron state density at the tails of the Se band edges, widen these tails into the band gap and, respectively, shift the absorption edge to lower energies. At high doping levels, the absorption of PbSe nanoparticles formed in the Se matrix can contribute significantly to the long-wavelength region of the spectrum.

The lead doping also has a pronounced effect on the action spectra of the films. Fig. 2(a) presents spectral dependences of the photocurrent quantum yield (Y) of the undoped and Pb-doped Se film electrodes recorded in 0.1 M HNO_3 solution. It should be noted that the long-wavelength edge of the photocurrent spectra is significantly shifted to higher energies as compared with that of the absorption spectra. A similar effect has been reported previously when comparing the absorption and photoconductivity spectra of sputtered Se films and assigned by a number of researchers [16,17] to the exciton absorption at the long-wavelength edge, which does not contribute to the action spectra. Doping lead in the Se films results in a significant decrease of the photocurrent quantum yield in the wide spectral region up to 550 nm, while a marked sub-bandgap photoresponce, manifesting itself as a photocurrent tail at $\lambda > 600$ nm, appears for the Se(Pb) films in contrast to the undoped ones (Fig. 2(b)). We have previously shown that the Pb adatoms at the Se surface are efficient recombination centers for the photogenerated charge carriers [15]. The formation of Pb–Se chemical bonds has been found to result in the appearance of a spectrum of electron surface states, which are located near the valence band edge and are capable of an efficient electron exchange with this band. The lead doping can result in the formation of a rather high density of such intra-bandgap states throughout the whole film bulk, which give rise to the recombination losses and, respectively, to the photocurrent drop. The fact that the spectrum of the photoelectrochemical activity of the Pb-doped electrodes is widened up to 1100 nm can be associated with inducing the electron transfers from these intra-bandgap states into the Se conduction band.

A sharp rise in the efficiency of the dark cathodic and anodic processes observed for the Se(Pb) electrodes in comparison to that for the Se ones can be also explained by the appearance of the intra-bandgap states, which efficiently exchange charge carriers with the valence band of Se. Therefore, the dark cathodic current associated with the H^+ reduction and the reduction of Se to H_2Se appears at more positive potentials (−0.2 V) for the Se(Pb) electrodes as compared with that for the Se ones (−0.3 V) (Fig. 3(a)). On the following potential scan in the positive direction, an anodic current related to the H_2Se oxidation is observed at the Se(Pb) electrodes and is absent at the Se ones. The efficiency of the cathodic processes in solutions containing different redox species, for example $Fe(CN)_6^{3-}/Fe(CN)_6^{4-}$ redox pair, also

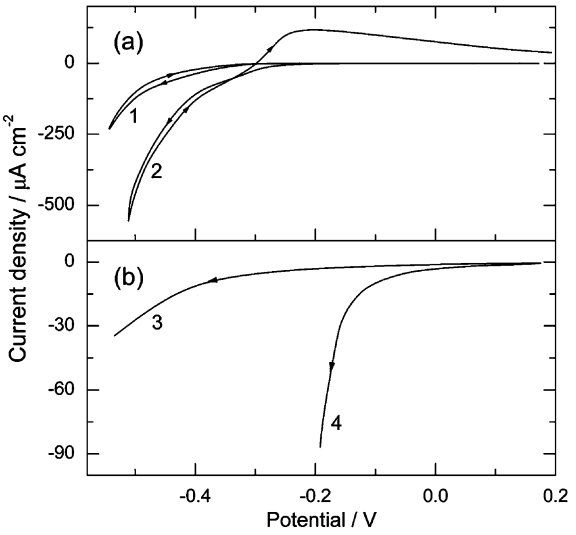

Fig. 3. Voltammograms of the undoped (1, 3) and Pb-doped (1 at.% Pb) Se film electrodes (2, 4). Electrolyte: (a) 0.1 M HNO_3; (b) 0.02 M $K_3[Fe(CN)_6] + 0.05$ M $K_4[Fe(CN)_6]$. Potential scan rate: 0.02 V s^{-1}.

increases drastically at the Se(Pb) electrodes (Fig. 3(b)).

3.4. Lead underpotential deposition onto Pb-doped Se films

Cyclic voltammograms of Se(Pb) electrodes with a Pb content of 1 at.% in Pb^{2+}-containing solution are shown in Fig. 4(a). It should be noted that the Pb UPD is feasible in the dark at the Se(Pb) electrodes in contrast to the Se ones and results in the appearance of a cathodic peak C_1 at −0.31 V (Fig. 4(a), curve 1). A related anodic peak A_1 associated with the Pb_{ad} oxidation is observed at 0.27 V. Repeated potential cycling between −0.4 and 0.4 V gives rise to a significant shift (by 0.25 V) of the peak C_1 to more positive potentials, indicating that the energy states of the Pb_{ad} at the Se(Pb) surface change significantly when cycling. The steady-state position of the peaks C_1 and A_1 after the repeated potential cycling coincides with the position of similar peaks of a PbSe electrode (Fig. 4(a), dashed line). This fact allows us to assume that a PbSe layer is formed on the Se(Pb) film surface on the potential cycling. We have previously shown that the conversion of a Pb_{ad} monolayer into PbSe on the Se surface is due to its chemical oxidation by Se and to the partial diffusion of the Pb_{ad} into the Se matrix [15]. The complete coincidence of the peak C_1 for the Se(Pb) films with that for the PbSe electrodes indicates that the PbSe layer is continuous. The formation of a discontinuous layer is less possible because in that case several peaks corresponding to different energy states of Pb_{ad} (Pb_{ad} on Se and Pb_{ad} on PbSe) would have been observed in the cathodic voltammograms.

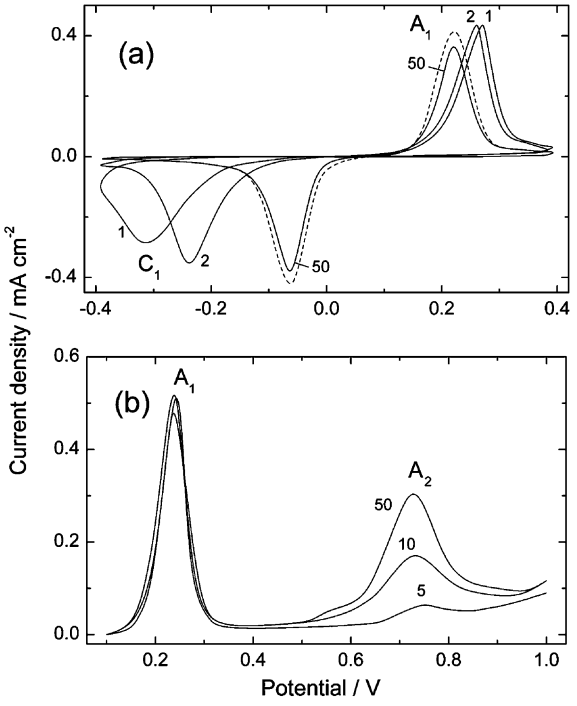

Fig. 4. (a) Cyclic voltammograms of Pb-doped Se film electrode (1 at.% Pb) (—) and PbSe film electrode (- - -) in 0.05 M $Pb(NO_3)_2$ + 0.1 M HNO_3 solution for the first, second and 50th potential scan. (b) Anodic voltammograms of the Pb-doped (1 at.% Pb) Se film measured under the same conditions after 5, 10, and 50 scans of potential between −0.4 and 0.4 V. Potential scan rate: 0.02 V s^{-1}.

The PbSe layer formed on the Se(Pb) surface can be readily identified electrochemically by the relevant oxidation peak A_2 observed when the potential is swept in the positive direction (Fig. 4(b)). The charge corresponding to this peak increases as the PbSe accumulates and finally reaches a limiting value of 500 μC cm^{-2}. This value indicates that the amount of PbSe formed on the Se(Pb) surface is rather small and can be estimated as several monolayers.

4. Conclusions

The use of the lead UPD onto selenium during the Se and Pb electrochemical co-deposition makes it possible to produce nanocomposite films consisting of the amorphous Se and nanosized PbSe clusters distributed throughout the film bulk. The lead doping strongly modifies the optical and photoelectrochemical properties of the Se films and significantly increases the efficiency of the charge transfer both in the film bulk and through the semiconductor | electrolyte interface. Owing to this modification, the Pb UPD onto the Se(Pb) surface in the dark, which does not occur on the

undoped selenium, can be realized, and additional submono- and monolayers of PbSe can be deposited on the Se(Pb) electrodes.

Acknowledgement

The work has been supported by the Basic Research Foundation of Belarus for financial support (grant X00M-098).

References

[1] Z. Loizos, N. Spyrellis, G. Maurin, Thin Solid Films 204 (1991) 139.
[2] B.W. Gregory, D.W. Suggs, J.L. Stickney, J. Electrochem. Soc. 138 (1991) 1279.
[3] L.P. Colletti, B.H. Flowers, J.L. Stickney, J. Electrochem. Soc. 145 (1998) 1442.
[4] I. Villegas, J.L. Stickney, J. Electrochem. Soc. 139 (1992) 686.
[5] A. Gichuhi, B.E. Boone, C. Shannon, Langmuir 15 (1999) 763.
[6] M.L. Foresti, G. Pezzatini, M. Cavallini, G. Aloisi, M. Innocenti, R. Guidelli, J. Phys. Chem. B 102 (1998) 7413.
[7] G. Pezzatini, S. Caporali, M. Innocenti, M.L. Foresti, J. Electroanal. Chem. 475 (1999) 164.
[8] S. Zou, M.J. Weaver, Chem. Phys. Lett. 312 (1999) 101.
[9] E.A. Streltsov, N.P. Osipovich, L.S. Ivashkevich, A.S. Lyakhov, V.V. Sviridov, Electrochim. Acta 43 (1998) 869.
[10] N.P. Osipovich, E.A. Streltsov, Rus. J. Electrochem. 36 (2002) 1.
[11] E.A. Streltsov, N.P. Osipovich, L.S. Ivashkevich, A.S. Lyakhov, Electrochim. Acta 44 (1998) 407.
[12] E.A. Streltsov, N.P. Osipovich, L.S. Ivashkevich, A.S. Lyakhov, Electrochim. Acta 44 (1999) 2645.
[13] T. Torimoto, K. Obayashi, S. Kuwabata, H. Yoneyma, Electrochem. Commun. 2 (2000) 359.
[14] T.L. Wade, R. Vaidyanathan, U. Happek, J.L. Stickney, J. Electroanal. Chem. 500 (2001) 322.
[15] E.A. Streltsov, S.K. Poznyak, N.P. Osipovich, J. Electroanal. Chem. 518 (2002) 103.
[16] N.F. Mott, E.A. Davis, Electron Processes in Non-crystalline Materials, Clarendon Press, Oxford, 1979.
[17] J.L. Hartke, P.J. Regensburger, Phys. Rev. 139 (1965) A970.